

4th CIRP Conference on Surface Integrity (CSI 2018)

Influence of rotational speed on surface states after stream finishing

Andreas Kacaras^{a,*}, Jens Gibmeier^b, Frederik Zanger^a, Volker Schulze^{a,b}

^a*Institute of Production Science, Karlsruhe Institute of Technology, Kaiserstr. 12, 76131 Karlsruhe, Germany*

^b*Institute for Applied Materials, Karlsruhe Institute of Technology, Kaiserstr. 12, 76131 Karlsruhe, Germany*

* Corresponding author. Tel.: +49-721-608-44015 ; fax: +49-721-608-45004. E-mail address: Andreas.Kacaras@kit.edu

Abstract

The stream finishing process proved to be an efficient production process for mechanical surface modification. In particular the rotational speed of a bowl containing the media represents an effective process variable for increasing relative velocity between workpiece and media. Increased work hardening effects and induced compressive residual stresses in the near surface region are expected. In this work the temporal influence of the rotational speed of the bowl on work hardening, residual stresses and surface topography are investigated on quenched and tempered AISI4140 plane specimen with the aim of determining the optimal processing time for surface modification. Furthermore, it is investigated whether grain refinement occurs during stream finishing. A modified Almen system is used as an efficient method for characterizing changes in residual stresses and surface topography during stream finishing. While depth ranges of residual stresses and work hardening showed to be affected by the rotational speed of the bowl and the processing time during stream finishing, residual stress states at the surface showed to be invariant. Increased process efficiency can be obtained by stream finishing using high rotational speed yielding higher depths of induced compressive residual stresses and work hardening in the near surface region in a shorter processing time.

© 2018 The Authors. Published by Elsevier Ltd. This is an open access article under the CC BY-NC-ND license

(<https://creativecommons.org/licenses/by-nc-nd/4.0/>)

Selection and peer-review under responsibility of the scientific committee of the 4th CIRP Conference on Surface Integrity (CSI 2018).

Keywords: Surface modification; Residual stress; Finishing

1. Introduction

Mass finishing processes are typically used for a defined setting of surface topography of complex shaped workpieces. However, only few scientific articles concern mass finishing processes for mechanical surface treatment with the aim of fatigue life enhancement or optimization of tribological properties of mechanical components. Here, the stream finishing process [1] and modified vibratory finishing processes [2,3,4,5] are focused. Feldmann et al. [2], Sangid et al. [3,4] and Hashimoto et al. [5] investigated modified vibratory finishing processes for surface modification and concluded their capability to induce significant compressive residual stresses into the near surface region accompanied by highly reduced surface roughness. Results show beneficial effects on run-in performance of treated functional surfaces on standard bearings made of carburized steel [5], on fatigue life of processed nickel based alloy parts [2] and friction coefficient of treated AISI52100 parts [5]. The stream finishing process shows higher relative flow velocities

between media and workpiece compared to the vibratory finishing process due to characteristic kinematics. Schulze et al. [1] demonstrated the stream finishing treatment to be a highly effective mass finishing process for mechanical surface modification focusing on the temporal evolution of surface states.

Increased impact velocity of the media on the workpiece's surface has great potential in inducing a higher amount of compressive residual stresses and causing greater work hardening into the near surface region accompanied by reduced finishing time for surface smoothing and thus for increased surface efficiency. A classification of mass finishing processes within other surface modification processes regarding tool characteristics and impact velocity is illustrated in Fig. 1 along with the potential of stream finishing using increased rotational speed. In this work the temporal influence of rotational speed on the residual stress state, work hardening, surface topography and grain refinement of quenched and tempered AISI4140 plane specimen during stream finishing is investigated.

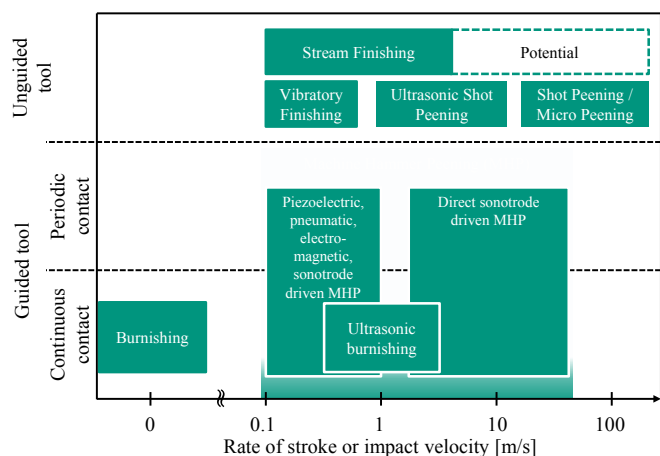


Fig. 1. Classification of surface modification processes modified from [6]. Values for vibratory finishing from [4] and for micro peening from [7].

Nomenclature

t	Processing time
n_i	Rotational speed of the bowl
h_i	Depth of immersion
r	Radius of immersion
F_N	Normal force
$F_{N,max}$	Maximum normal force
$F_{N,s}$	Normal force in stationary state
p_N	Normal pressure
H	Arc height
Sa	Arithmetic average surface roughness
Str	Texture aspect ratio
Δm	Mass difference
c	Coverage
f	Frequency of impacts
A_{impact}	Impact area of a particle
A_{total}	Processed surface area
a_p	Edge length of an idealized particle
v_p	Relative velocity between workpiece and media
σ_{RS}^{long}	Residual stress in longitudinal direction
x	Depth
Δ/B	Integral breadth difference compared to initial state

2. Experimental

For experiments a prototypical stream finishing machine (Otec Präzisionsfinish GmbH) capable of realizing high processing intensities due to high rotational speed of the bowl was used. A high density sintered alumina ceramic KXMA 16 with an average grain size of 1.7 to 2.4 mm with water and compound SC15 served as media. The workpiece was vertically immersed into the media (Fig. 2). Rotational movement of the bowl causes medium flow around the workpiece leading to the processing effect. It is known, that greater impact velocities lead to more plastic deformation which can be achieved by increasing rotational speed n of the bowl. In this work the rotational speed n was varied within the range of 76 min^{-1} to 600 min^{-1} in order to study the temporal influence of increased rotational speed on surface states. The processing time t was varied within the range of 5 s to 10 min.

Processing times greater than 10 min were not considered since [1] proved surface states to be almost stationary after 3.75 min using $n = 70 \text{ min}^{-1}$. The maximum radius of immersion r possible was chosen in order to achieve the maximum relative speed between workpiece and media during processing. Higher centrifugal forces caused by higher rotational speeds lead to a specific geometrical distribution of the media inside the bowl. Depths of immersion h_i were approximated on the basis of video captures of the media and ablated black ink which was applied to the workpiece holder before processing. Table 1 shows the predefined processing parameters which were kept constant.

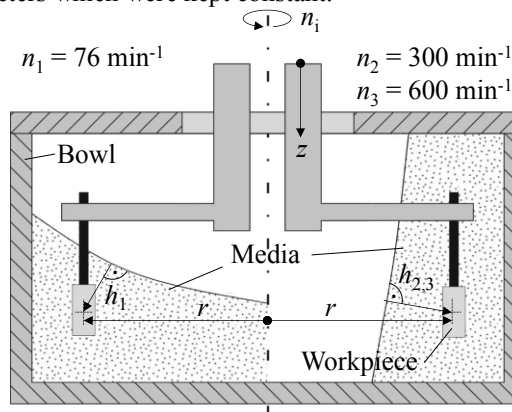


Fig. 2. Schematic view of the prototypical stream finishing machine.

Table 1. Constant processing parameters.

Processing parameter	Value
Depth of immersion h_1	~40 mm
Depth of immersion $h_{2,3}$	~70 mm
Radius of immersion r	250 mm

Previous studies [1] proved the Almen system [8] to be suitable for efficient characterization of change in residual stress state using adapted Almen strips during stream finishing and thus were used within this work. Three specimen (dimensions 25.4 mm x 3.175 mm x 0.79 mm) were prepared, processed and analyzed for each parameter configuration. Workpiece material was AISI4140 (EN steel 1.7225) in a quenched and tempered state (austenized at 850°C , quenched in oil and tempered at 450°C for 2 h). Heat treatment of the adapted Almen strips was performed after surface grinding leading to a balanced residual stress state with a value of almost 0 MPa. Longitudinal grooves on the workpiece's surface (Fig. 3), with an initial surface roughness of approximately $Sa = 0.33 \mu\text{m}$, were caused by the surface grinding process.

After the finishing treatment arc height H , arithmetic average surface roughness Sa , texture aspect ratio Str as well as mass change Δm were evaluated for each adapted Almen strip analogously to [1]. In order to determine the stationarity of the media's flow state temporal evolution of normal force F_N was measured during finishing using a piezo resistive force sensor (FlexiForce A201, force range 0-111 N, Tekscan Inc.) attached to the workpiece holder. The force signals were amplified and digitized at 10 Hz. A linear curve fit was used for calibration of the sensor. Comparable sensor equipment was proved to be suitable for investigating contact forces

during vibratory finishing by Yabuki et al. [9]. Residual stress depth distributions were analyzed by X-ray stress analysis analogously to [1] but only in longitudinal direction since [1] showed the magnitude of surface residual stresses in transverse and longitudinal directions to be comparable after stream finishing. For each condition selected one specimen was analyzed. A primary aperture with a nominal diameter of 1 mm was used. Integral breadths IB of the diffraction lines served to assess the stream finishing process' cold working effect. Qualitative evaluation of grain refinement within the workpiece's near surface region after machining was undertaken using a Focused Ion Beam (FIB) system.

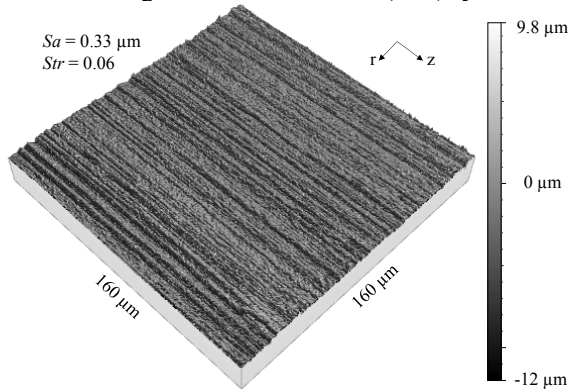


Fig. 3. Initial surface topography after surface grinding.

3. Results and Discussion

3.1. Evaluation of normal forces

Figure 4 shows the temporal evolution of normal force and its weighted moving average (sample window of 20) during stream finishing using rotational speeds $n = 76 \text{ min}^{-1}$ and $n = 300 \text{ min}^{-1}$. Occurring strong abrasive effects on the sensor lead to sensor damage and thus prevented from force signal acquisition during processing at $n = 600 \text{ min}^{-1}$.

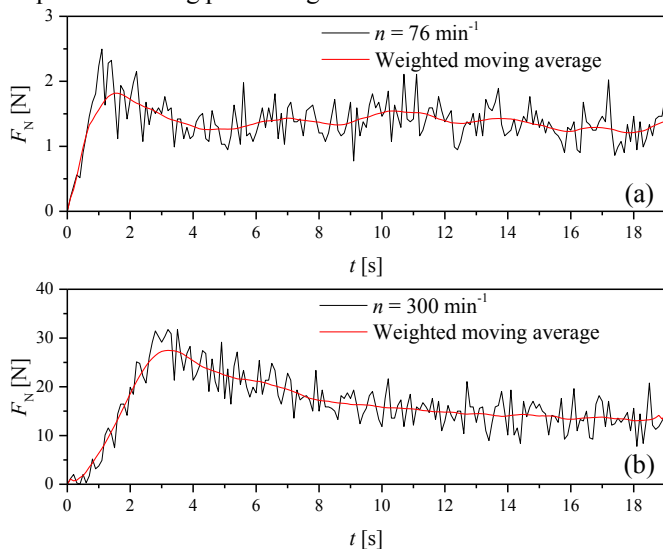


Fig. 4. Temporal evolution of normal forces and its weighted moving average during stream finishing using rotational speeds (a) 76 min^{-1} and (b) 300 min^{-1} .

With acceleration of the rotational speed of the bowl an increase of normal force F_N is observed until the targeted

rotational speed is reached. Here, maximum normal forces of nearly $F_{N,max} = 2.5 \text{ N}$ for $n = 76 \text{ min}^{-1}$ and $F_{N,max} = 32 \text{ N}$ for $n = 300 \text{ min}^{-1}$ were observed. Normal forces decline during the course of time after $F_{N,max}$ until a stationary state $F_{N,s}$ is reached. This is caused by a delayed stationary flow state of the media. $F_{N,s,76} = 1.35 \text{ N}$ and $F_{N,s,300} = 15 \text{ N}$ is reached after approximately 5 s for $n = 76 \text{ min}^{-1}$ and 12 s for $n = 300 \text{ min}^{-1}$. Higher rotational speeds lead to increased impoundment effects within the media requiring longer times until stationary flow states are reached. Further, a growing ratio of $F_{N,max} / F_{N,s}$ can be observed. Figure 5 displays the measured and expected normal pressures during stream finishing.

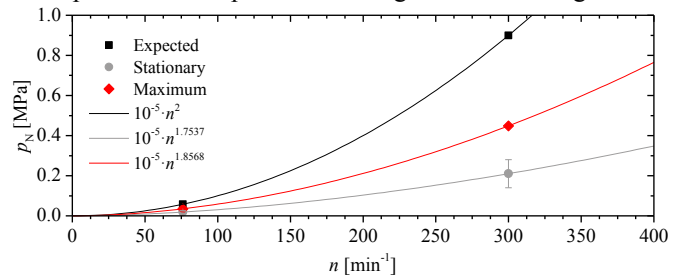


Fig. 5. Measured and expected normal pressures and applied curve fits during stream finishing using rotational speeds 76 min^{-1} and 300 min^{-1} .

Given that a particle's kinetic energy determines the normal force measured on a workpiece surface a quadratic relation $p_N \sim n^2$ is expected. However, results of the curve fits show slightly lower correlation exponents. Impoundment effects within the media lead to a reduction of relative velocity between workpiece and media. Hence, a reduced kinetic energy due to increasing impoundment effects associated with an increase in rotational speed n seems to be responsible for the less than quadratic relation between n and p_N .

3.2. Arc height and surface topography

The amount of work absorbed by the workpiece surface induced by a particle impact is less than the initial particle's kinetic energy [10] and results in plastic deformation of the workpiece's near surface region. Plastic deformation usually is accompanied by work hardening effects and the induction of compressive residual stresses into the near surface region. The arc height H of a processed Almen strip characterizes the change in residual stress state within the affected near surface region qualitatively. Arc heights of the processed adapted Almen strips were measured analogously to [1].

Figure 6 (a) displays the temporal evolution of arc heights during stream finishing for different rotational speeds. Strong abrasive effects during stream finishing using a rotational speed of $n = 600 \text{ min}^{-1}$ prevented from measuring arc heights longer than a finishing time of 30 s. During the first 10 s of processing time the most significant increase in arc heights can be obtained for all tested rotational speeds. For further processing a slight increase of arc heights can be obtained reaching an almost stationary state after approximately 3 min for the rotational speeds $n = 76 \text{ min}^{-1}$ and $n = 300 \text{ min}^{-1}$ indicating that no significant additional compressive residual stresses will be induced. Comparing the magnitude of measured arc heights after a processing time of 30 s an almost

linear relation between the rotational speed and the resulting arc height $H \sim n$ can be derived which is skipped here due to available space.

Figure 6 (c,d) depict the temporal evolution of mass difference Δm and arithmetic average surface roughness Sa resulting from abrasive effects during stream finishing.

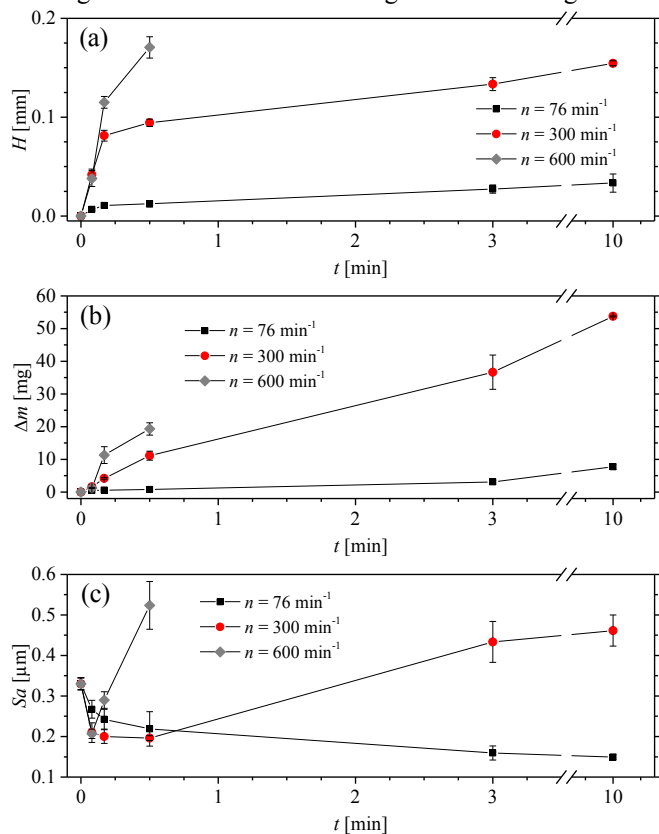


Fig. 6. Temporal evolution of (a) arc height, (b) mass difference and (c) surface roughness during stream finishing.

In accordance to Schulze et al. [1] a stationary roughness state with approximately $Sa = 0.15 \mu\text{m}$ is reached between a processing time of 30 s to 3 min for a rotational speed of $n = 76 \text{ min}^{-1}$. Consequently, the mathematical roughness prediction model established by Hashimoto et al. [11] can be applied. Using high rotational speed roughness change occurs with local roughness minima at approximately $Sa = 0.2 \mu\text{m}$ after 5 s to 30 s for $n = 300 \text{ min}^{-1}$ and 5 s for $n = 600 \text{ min}^{-1}$. Further processing leads to a significant increase of roughness in both cases exceeding the initial surface roughness. Using a rotational speed of $n = 300 \text{ min}^{-1}$ an almost stationary roughness state of approximately $Sa = 0.44 \mu\text{m}$ can be observed after 3 min of finishing time. A dependency of the stationary roughness value on the rotational speed can be stated. Higher normal pressure (Fig. 5) leads to an increased intensity of media-workpiece impacts resulting in an increased stationary roughness value. This can affect workpiece fatigue life detrimentally. After roughness change micro cutting mechanisms occur as can be seen from a lower progression of mass difference. Based on these findings the mathematical roughness prediction model by [11] is not applicable for the stream finishing process at high rotational speeds.

The initial spatial anisotropic surface topography related to the grooves caused by surface grinding with a preferred texture direction in the z -direction (Fig. 3) leads to an initial low texture aspect ratio of $Str = 0.06$. After a finishing time of 30 s using $n = 76 \text{ min}^{-1}$ a stationary state of texture aspect ratio with $Str = 0.72$ is reached implying a surface topography without oriented structures. Using high rotational speed oriented structures are removed after a finishing time of 5 s due to occurring higher abrasive effects (Fig. 6 (b)).

3.3. Evaluation of coverage

The coverage c defining the ratio between the impacted area by impinging particles and the treated surface area affects the residual stress state of the near surface region during vibrostrengthening [4]. Sangid et al. [4] applied and experimentally validated the stochastic model given in Eq. 1 in order to describe the relationship between the coverage c and the corresponding processing time t .

$$t = - \frac{\ln(1-c)}{f \cdot A_{\text{impact}} / A_{\text{total}}} \quad (1)$$

The frequency of impacts is described by f and the expected coverage area of a single particle impacting the workpiece by $A_{\text{impact}}/A_{\text{total}}$.

In order to induce compressive residual stresses into a workpiece surface homogeneous and high coverage is needed. Achieving high coverage quickly increases process efficiency. Eq. 1 was applied to the studied process in order to evaluate the significance of reduced processing time needed to reach high coverage by high rotational speed. The dimensions of the particles used are undefined and thus were idealized as cubes with an edge length a_p of 1.47 mm. a_p represents the average value of maximum and minimum dimensions of 100 measured particles using an outside micrometer. The average particle dimension was found to be a bit smaller than declared in the data sheet (Section 2). The processed surface area A_{total} measured 80.65 mm². The rotational velocity $2\pi nr$ was assumed for particle velocity v_p . The particle impact area A_{impact} was idealized by an elliptical shape derived from light microscopic images of processed workpieces. Ideal packing of the media was assumed. Specific parameters are displayed in Table 2.

Table 2. Parameters used in Eq. 1.

Parameter	$n = 76 \text{ min}^{-1}$	$n = 300 \text{ min}^{-1}$	$n = 600 \text{ min}^{-1}$
v_p [m/s]	1.99	7.85	15.71
A_{impact} [mm ²]	1.50 E-05	2.15 E-05	3.16 E-05
f [1/s]	50059	197471	395194
$A_{\text{impact}}/A_{\text{total}}$ [-]	1.86 E-07	2.66 E-07	3.92 E-07
c after 3 min [%]	81	99.99	≈100
t for $c = 99\%$ [min]	8.26	1.46	0.5

A stationary arc height state can only be seen along with a high impact coverage. Almost stationary arc height values after 3 min of stream finishing using $n = 76 \text{ min}^{-1}$ and $n = 300 \text{ min}^{-1}$ (Fig. 6 (a)) and corresponding calculated coverages are in accordance to this. The calculated processing

time of 30 s needed to reach a coverage of 99% using $n = 600 \text{ min}^{-1}$ indicates that no significant increase of arc height and thus no significant additional compressive residual stresses will be induced after this time.

Further investigations are needed for a better description of the occurring media velocity affecting the workpiece surface during stream finishing and the experimental validation of calculated coverages. A significant reduction in processing time necessary for attaining high coverage using high rotational speed can be derived from Table 2. Thus, process efficiency for surface modification by stream finishing can be ameliorated using high rotational speed.

3.4. Residual stress states and work hardening

In order to evaluate the influence of rotational speed on the residual stress state and work hardening the conditions were selected showing significant change in residual stress state evaluated by arc heights (Fig. 6a) and showing a stationary texture aspect ratio Str . For evaluating the influence of processing time on the residual stress state and work hardening the rotational speed was kept constant at 300 min^{-1} with varying processing time.

Figure 7 depicts the depth distributions of residual stresses in longitudinal direction for the initial state before processing as well as after finishing using different rotational speeds and finishing times.

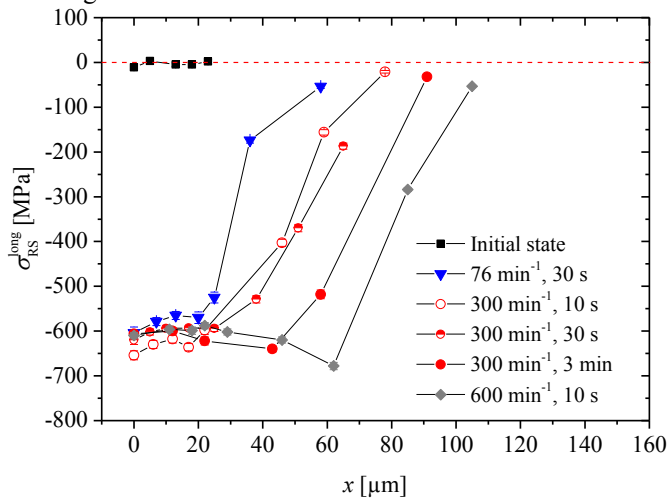


Fig. 7. Depth distributions of the residual stresses after stream finishing.

Significant induced surface compressive residual stresses can be obtained after stream finishing showing comparable magnitudes of -600 to -660 MPa . Hence, surface residual stress states were found to be almost invariant to n and t . The depth range of compressive residual stresses increases from nearly $60 \mu\text{m}$ for $n = 76 \text{ min}^{-1}$ at 30 s to approximately $100 \mu\text{m}$ for $n = 600 \text{ min}^{-1}$ at 10 s. Comparing residual stress depth distributions with constant processing time but increasing rotational speed, a significant increase of the depth range of compressive residual stresses is found. If t is varied at constant n again depth range is increasing. Comparing the resulting residual stress states to the results of Weingärtner et al. [7] studying micro peening, surface compressive residual stresses prove to be in a similar range – obviously also

without a clear tendency with increasing intensity – while a slightly higher depth range can be achieved by stream finishing. Assessing the results for residual stress depth distribution using $n = 600 \text{ min}^{-1}$ at 10 s, an increase of compressive residual stress of nearly $\Delta\sigma_{RS}^{\text{long}} = 70 \text{ MPa}$ up to a depth range of $60 \mu\text{m}$ can be seen suggesting an increasing influence of Hertzian stress with higher n due to increased p_N .

Relating these findings to the results of Sangid et al. [3] it becomes evident that the effect of Hertzian stress is important for both processes, the vibrostrengthening and the stream finishing, the later also showing effects of plastic stretching due to tangential forces during abrasion. The findings in Fig. 7 can roughly be explained in a first approach as follows. A particle impact causes plastic deformation on the workpiece surface and thus induces compressive residual stresses into the impacted area. It is known from [12] that the stresses within a single impact are much higher as the more equilibrated stresses after reaching full coverage. The same holds for the depth distributions of the residual stresses. During X-ray analysis, the residual stress is determined over an area arising from the used aperture which is much higher than a single impact. Consequently, measured residual stresses measured at very low coverages like after finishing using rotational speeds $n = 76 \text{ min}^{-1}$ and $n = 300 \text{ min}^{-1}$ at 10 s are averaged values of quite high central compressive stresses in the impacts and tensile values in the surrounding. At high coverages like in the other depth distributions shown, this is already equilibrated on a homogeneous compressive level. Therefore the independence of residual stresses at the surface and within the first $40 \mu\text{m}$ can be understood from measurement and coverage.

Depth distributions of the integral breadths used as a value for assessing work hardening effects are illustrated in Fig. 8. With increasing time and rotational speed the integral breadths and their depth distribution increase as expected.

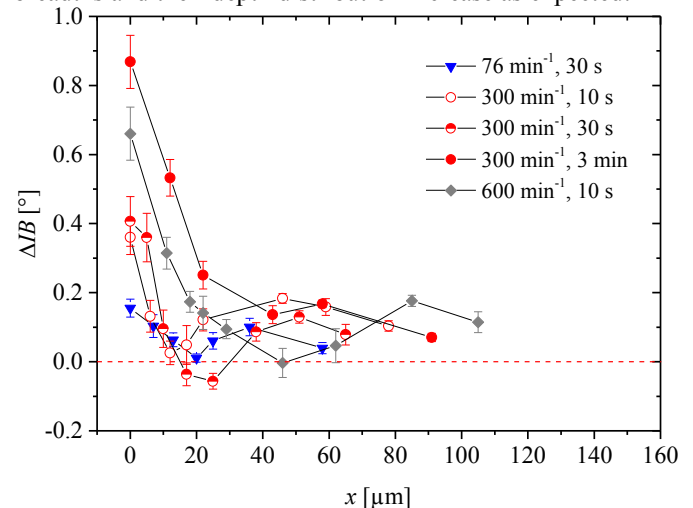


Fig. 8. Depth distributions of the integral breadths after stream finishing.

An unexpected higher amount of work hardening can be obtained after finishing using $n = 300 \text{ min}^{-1}$ at 3 min compared to $n = 600 \text{ min}^{-1}$ at 10 s. Increasing n is accompanied by a growing intensity in abrasive effects. Consequently, due to the increased material removal rate (Fig. 6 (b)) strain softening effects may occur in the near

surface region. In comparison to micro peened parts by [7] higher depth ranges of work hardening effects can be achieved through stream finishing. Presently, it is still not understood, why the depth distributions of integral breadths and compressive residual stresses are differing in their dependence on process parameters. This needs further studies.

3.5. Grain refinement

In order to investigate whether grain refinement occurs during stream finishing a FIB image analysis was undertaken in radial direction (Fig. 9) for a single condition exemplarily. Here, the part showing maximum induced work hardening (Fig. 8) was analyzed. Significant grain refinement can be observed in the near surface region down to a depth of 1 μm . Furthermore, plastic stretching effects can be observed in a depth range of 1 μm to 3 μm . These may be caused by occurring tangential forces during abrasion. The quantitative evaluation of grain refinement under specific conditions will be part of future work.

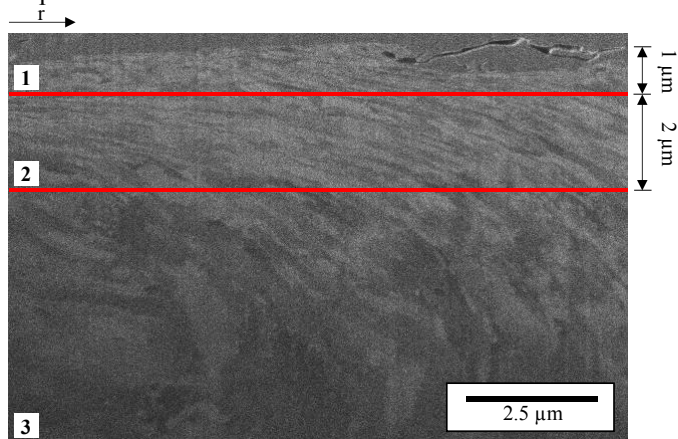


Fig. 9. FIB image of the surface layer after stream finishing using 300 min^{-1} at 3 min. 1 grain refinement, 2 plastic stretching, 3 bulk material.

4. Conclusion

The potential of improving process efficiency for surface modification during stream finishing using increased rotational speed was investigated. Results of the temporal influence of rotational speed on the surface states of quenched and tempered AISI4140 plane specimen show the feasibility of reducing surface smoothing processing time accompanied by increased induced compressive residual stresses and work hardening into the near surface region. From this work following key findings can be derived:

- While depth ranges of induced compressive residual stresses (60 to 100 μm) and work hardening (40 to 90 μm) showed to be affected by the rotational speed of the bowl and the processing time during stream finishing, surface residual stress states showed to be almost invariant ranging from -600 to -660 MPa.
- Surface smoothing effect is followed by a significant increase of roughness after a specific finishing time using $n = 300 \text{ min}^{-1}$ and $n = 600 \text{ min}^{-1}$ and reaches a stationary roughness state. This is in contrast to the results using $n = 76 \text{ min}^{-1}$ showing converging roughness value. A

correlation between increased stationary surface roughness and rotational speed can be stated.

- Aiming at the best possible surface smoothing effect longer processing times generating a stationary residual stress state analogously to [1] are not expedient for the rotational speeds $n = 300 \text{ min}^{-1}$ and $n = 600 \text{ min}^{-1}$ due to the obtained increase in surface roughness.
- FIB analysis proves the capability in significant grain refinement due to plastic stretching effects.
- Occurring in-process normal pressures on the workpiece surface show a non-proportional relationship to the media's kinetic energy and thus differ from expectations. Impoundment effects are related to this finding.
- Coverages were calculated by a stochastic model. A significant reduction in processing time for the attainment of high coverage using high rotational speed can be derived. Further investigations are needed for a better description of the occurring media velocity and the experimental validation of calculated coverages.

Acknowledgements

All authors acknowledge the financial support provided by the German Federation of Industrial Research Associations (AiF). The partner Otec Präzisionsfinish GmbH supported this project generously.

References

- [1] Schulze V, Gibmeier J, Kacaras A. Qualification of the stream finishing process for surface modification. *CIRP Ann-Manuf Techn* 2017; 66(1): 523-526.
- [2] Feldmann G, Haubold T, Wong CC, Wei W. Application of vibropeening on Aero-Engine Component. *Procedia CIRP* 2014;13:423-428.
- [3] Sangid MD, Stori JA, Ferriera PM. Process characterization of vibrostrengthening and application to fatigue enhancement of aluminium aerospace components – part I. Experimental study of process parameters. *Int J Adv Manuf Technol* 2011;53:545-560.
- [4] Sangid MD, Stori JA, Ferriera PM. Process characterization of vibrostrengthening and application to fatigue enhancement of aluminium aerospace components – part II. Process visualization and modelling. *Int J Adv Manuf Technol* 2011; 53:561-575.
- [5] Hashimoto F, Chaudhari RG, Melkote SN. Characteristics and Performance of surfaces created by Various Finishing Methods (Invited Paper). *Procedia CIRP* 2016;45:1-6.
- [6] Schulze V, Bleicher F, Groche P, Guo YB, Pyun YS. Surface modification by machine hammer peening and burnishing. *CIRP Ann-Manuf Techn* 2016;65:809-832.
- [7] Weingärtner R, Hoffmeister J, Schulze V. Investigation on the Mechanism Improving Fatigue Strength in Surface Layers after Micropeening. Proceedings of the 12th International Conference on Shot Peening, Goslar, Germany, Sept. 15 – 18, ISBN 978-3-00-047738-6, 2014;31 – 36.
- [8] Almen JO. Shot blasting test. 1944, Serial No. 410987.
- [9] Yabuki A, Baghbanan MR, Spelt JK. Contact forces and mechanisms in a vibratory finisher. *Wear* 2002;252:635-643.
- [10] Ciampini D, Papini M, Spelt JK. Modeling the development of Almen strip curvature in vibratory finishing. *J Mater Process Tech* 2009; 209: 2923-2939.
- [11] Hashimoto F, DeBra DB. Modelling and Optimization of Vibratory Finishing Process. *Annals of the CIRP* 1996;45:303-306.
- [12] Schwarzer J, Schulze V, Vöhringer O. Finite element simulation of shot peening – A method to evaluate the influence of peening parameters on surface characteristics. L. Wagner, Proceedings of the 8th International Conference on Shot Peening ICSP 8, Garmisch-Partenkirchen 2002;507-515.